

Chapter 34

High-temperature membranes

J. S. Wainright, M. H. Litt and R. F. Savinell

Case Western Reserve University, Cleveland, OH, USA

1 INTRODUCTION

In recent years, there has been intense research interest in the development of proton electrolyte membrane (PEM) fuel cells for transportation and portable power applications. Typically, the polymer electrolyte used is a hydrated perfluorosulfonic acid polymer such as DuPont's Nafion[®]. This type of polymer requires water for proton conductivity; therefore, the operating temperature is limited to below the boiling point of water. The maximum conductivity of Nafion[®] occurs at 100% relative humidity (RH) and is practically constant with respect to temperature.^[1] Although operation at higher pressure can extend the operating temperature range, polytetrafluoroethylene (PTFE)-based materials, such as Nafion[®], have a maximum operating temperature limited by the physical properties of the material itself. Fuel cell operation at high current densities is complicated by the water drag accompanying proton transport. A water transport imbalance results, leading to dehydration near the anode and cathode flooding with liquid water.^[2] This is a significant engineering issue, which could be ameliorated with a water-starved proton conduction mechanism, as would be necessary in a high-temperature polymer electrolyte. This chapter addresses the research activities in the development of a high-temperature polymer electrolyte for fuel cell applications.

There are a number of reasons why a high-temperature polymer electrolyte would be useful besides lessening the problems associated with water drag. Consider the advantage of liquid fuels in terms of their energy density. These fuels are often difficult to oxidize directly in a fuel cell, except perhaps at very high temperatures. Thus, they need

to be reformed to produce H₂ and CO₂. The reforming reaction, which for kinetic reasons is run at a higher temperature, yields significant amounts of CO, driven by chemical equilibrium with CO₂ and water. Carbon monoxide severely poisons the platinum catalyst in a conventional PEM fuel cell.^[3] To deal with this, additional shift reactors and partial oxidation reactors are required to reduce the levels of CO to tolerable, i.e., low ppm, levels. The CO tolerance of a fuel cell can be greatly increased by elevating its operating temperature. For example, experiments in our laboratory have shown that a fuel cell operating at 150 °C can tolerate ca. 1% of CO with only minimal loss in cell voltage. Similar results are well known in the phosphoric acid fuel cell community. A theoretical calculation of CO coverage on Pt as a function of temperature and CO concentration has recently been presented.^[4] The greater CO tolerance at higher temperatures also results in lowering the necessary platinum loading to levels that have been found to give high performance on neat hydrogen. Greater CO tolerance also avoids the need for Pt alloy catalysts, which may be more expensive and less stable than pure Pt.

Operating a fuel cell at higher operating temperatures, for example 130 °C instead of 80 °C, also reduces the heat exchange area needed to dissipate excess heat. This could be a significant system advantage (perhaps a necessity) for the overall fuel cell system design. A polymer capable of proton conduction at 200 °C also opens up the possibility of directly coupling endothermic methanol reforming with the overall exothermic fuel cell reactions. This could lead to efficient energy integration and reduced size and complexity of the overall fuel cell system.^[5]

There is also increasing interest in the development of a direct methanol/air polymer electrolyte fuel cell (DMFC). DMFC operation at temperatures above 100 °C should improve electrode kinetics, improve tolerance to catalyst poisons, and reduce fuel crossover, especially if the methanol and water reactants are in the vapor phase.

In this chapter, we will summarize some of the reported accomplishments towards developing proton-conducting polymers capable of operating at elevated temperatures where water retention becomes an issue. The major emphasis in this discussion will be given to published and previously unpublished results obtained with the PBI/phosphoric acid system.

2 GENERAL APPROACHES

Several approaches have been pursued in the development of a high-temperature membrane for fuel cell applications. One approach is to modify a perfluorinated sulfonic acid membrane such as Nafion[®] by imbibing the membrane with a second substance such as SiO₂, which could retain water at higher temperature. Only nominal conductivity enhancement has been reported using this approach, although mechanical properties are improved with small amounts of SiO₂ addition.^[6, 7] Fuel cell results using a SiO₂/Nafion[®] membrane reported by Lee *et al.*^[8] suggest that improved conductivities are possible with this approach. A composite membrane of Nafion[®]/zirconium phosphate (Nafion[®] 115, protons exchanged with Zr⁴⁺, followed by precipitation in H₃PO₄) was reported to have an areal resistance of 0.12 Ω cm² at 90 °C, and decreased to 0.08 Ω cm² at temperatures of 140–150 °C in contact with an aqueous 2 M methanol solution at 4 atm pressure.^[9] These resistances indicate a conductivity of the order of 0.2 S cm⁻¹. In this system the zirconium phosphate increased the dry weight of Nafion[®] by 23% and the dry thickness by 30%. The zirconium phosphate, thought to be responsible for water retention, was estimated to have a particle size of about 11 nm, slightly larger than the pores in Nafion[®].

In another similar approach, the imbibed species is meant to replace water by solvating the proton to allow charge migration. The work of Savinell *et al.*^[10] demonstrated Nafion[®] proton conductivity at temperatures exceeding 100 °C when phosphoric acid was imbibed into the membrane. There were suggestions that the strong sulfonic acid groups of Nafion[®] protonated the more basic phosphoric acid.^[11] However, in unpublished work from this group, the Nafion[®]/phosphoric acid system could not sustain large current densities in an operating hydrogen/oxygen fuel cell. Although the reason is still unclear, a possible mechanism

may be anion migration, thus leading to excess phosphoric acid accumulation at the anode and consequent flooding of the electrode structure.

A third approach is based on using basic polymers that can absorb acids. If the absorbed acids are polyvalent oxo acids, then proton conduction can be through a Grotthuss mechanism; thus water is not needed for proton migration. The polybenzimidazole (PBI)/phosphoric acid system was introduced by Savinell and co-workers^[12, 13] and has received the most attention;^[12–26] therefore, a more detailed discussion of the reported results of this system and the closely related AB-PBI/phosphoric acid system will be given here.

2.1 PBI and AB-PBI

PBI is commercially manufactured by Hoechst-Celanese primarily for use in fabrics for fire protection clothing. The polymer is high-temperature resistant and chemically stable. It has a glass transition temperature of about 450 °C because of its all-aromatic structure. The benzimidazole group has a pK_a of about 5.5, which facilitates its absorption of acid, which can act as a plasticizer. The structure of PBI is shown in Figure 1. AB-PBI, not commercially available, has a chemical structure similar to PBI, but without the connecting phenyl group, as shown in Figure 2.

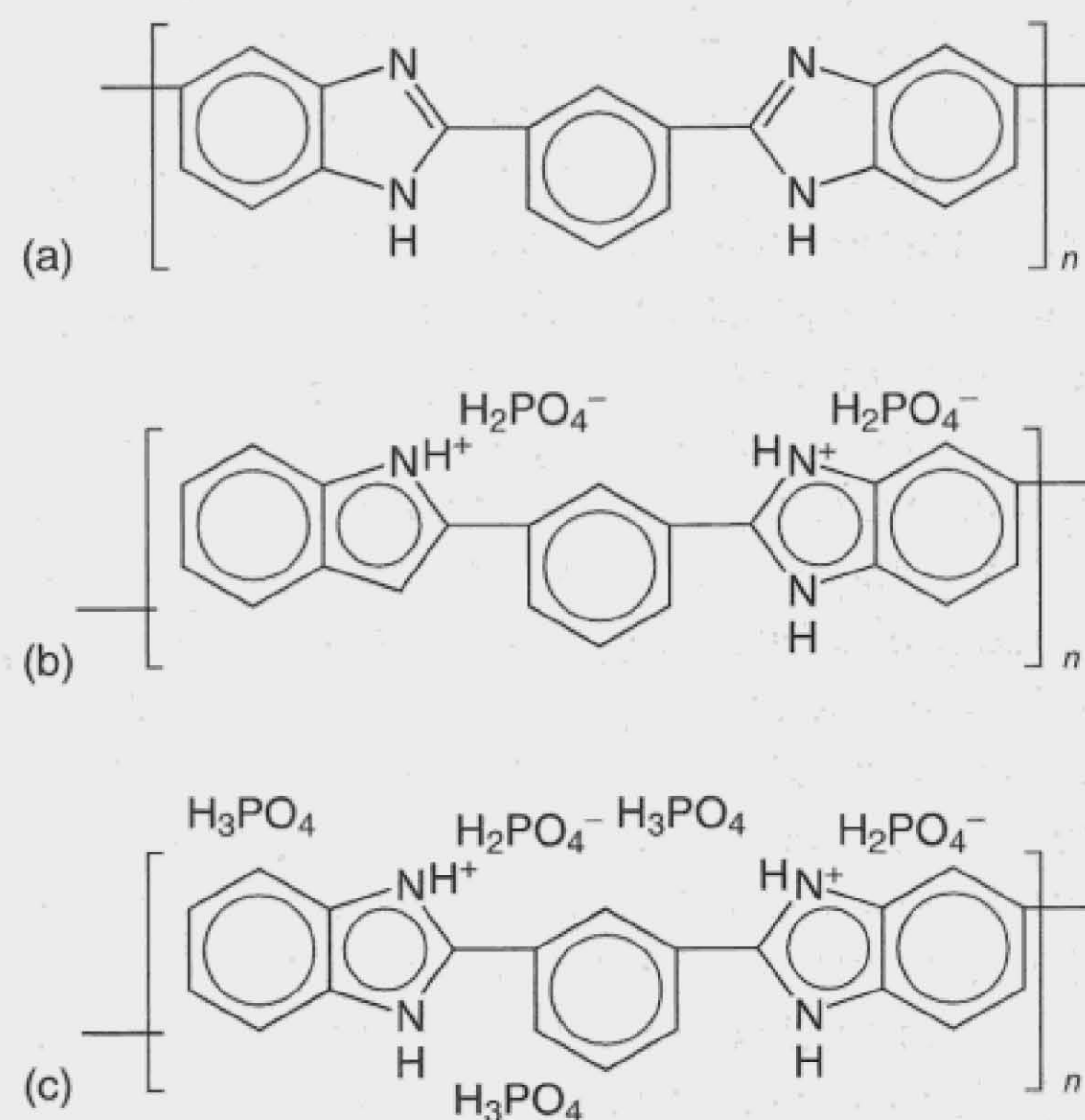


Figure 1. Structures of (a) polybenzimidazole (PBI), (b) PBI doped with 2 mol of phosphoric acid per repeat unit, and (c) PBI doped with 5 mol of phosphoric acid per repeat unit.

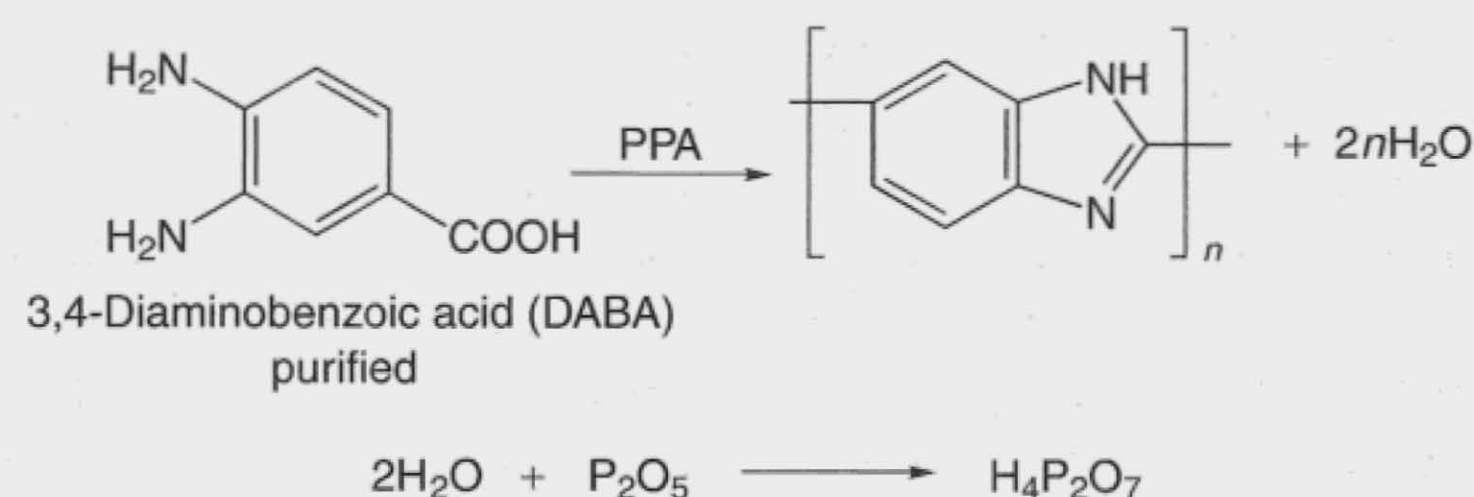


Figure 2. Scheme of synthesis AB-PBI.

2.2 PBI powder and acid doping

PBI polymer can be synthesized with a broad range of molecular weights. One measurement often used to characterize the molecular weight of a polymer is the inherent viscosity (IV). The IV is found by measuring the viscosity of a 0.5 wt% solution of the polymer dissolved in a solvent (concentrated sulfuric acid for PBI). The equation for calculating the IV is

$$\text{IV} = \frac{\ln(\text{flow time of the solution} / \text{flow time of the solvent})}{\text{solution concentration in g dl}^{-1}} \quad (1)$$

Table 1 shows the IV and molecular weight distribution for low, medium, and high molecular weight polymer. The low molecular weight material was purchased from Aldrich. Hoechst-Celanese usually makes medium molecular weight with an IV of ca. 0.7, but some high molecular weight material with an IV of about 0.91 has been made available. As will be shown later, high molecular weight material is necessary if the film is to have acceptable mechanical properties. Polymer with an IV of 0.3 could not form freestanding films. Our understanding is that the high-IV material is currently a byproduct in PBI manufacturing, but could be the primary product via process adjustments.

In order to increase the average molecular weight of polymer to produce high-quality films, the lower molecular weight components can be extracted by fractionation in dimethylacetamide (DMAc). Typical extraction results for

Table 1. Molecular weight and inherent viscosity of commercially available PBI^a.

Polymer	IV (dl g ⁻¹) ^b	M_n	M_w	MWD (M_w/M_n)
Low	0.3	6700	11 200	1.7
Medium	0.68	18 000	27 200	1.5
High	0.97	26 300	50 300	1.9

^a M_n , number-average molecular weight; M_w , weight-average molecular weight; MWD, molecular weight distribution (polydispersity index).

^bAll IV values for 0.5 wt% solution in sulfuric acid, 1 dl g⁻¹ = 0.11 g⁻¹.

the yield of undissolved polymer are shown in Table 2. For example, when material initially having IV = 0.91 is extracted at 94 °C, 69% of the original material remains with an IV of 1.14. The yield decreases as the average molecular weight of the material after extraction increases. The yield of these high-IV fractions would be significantly less for a starting material of IV = 0.71.

Owing to the basic nature of the benzimidazole group, PBI readily absorbs acid. Oxo acids are required to achieve proton conductivities commensurate with fuel cell operation. Primarily sulfuric and phosphoric acid doping has been considered. ³¹P nuclear magnetic resonance (NMR) experiments in our laboratory indicate that the first two phosphoric acids per repeat unit protonate the two benzimidazole groups, as shown in Figure 1(b). However, additional phosphoric acid is needed for high levels of conductivity, e.g., five acid molecules per repeat unit as shown in Figure 1(c). Bouchet and Siebert^[14] performed infrared (IR) studies and concluded that both sulfuric acid and phosphoric acid protonate the -C=N- of the imidazoles. In the case of sulfuric acid, full protonation occurred with one acid per repeat unit. The predominant species detected was SO₄²⁻ when $n < 0.6$, HSO₄⁻ when $0.6 < n < 1.5$, and H₂SO₄ when $n > 1.5$, where n = sulfuric acid per repeat unit. In the case of phosphoric acid, full protonation occurs at $n = 2$, and H₂PO₄⁻ was the predominant species over the concentration range studied. The IR studies of Kawahar^[15] gave similar conclusions for doped acids H₂SO₄, CH₃SO₃H,

Table 2. PBI extraction results using DMAc^a (initial IV = 0.91).

Trial	Fractionation temperature (°C)	Yield of undissolved polymer (%)	IV of undissolved polymer (dl g ⁻¹)
A	94	69	1.14
B	110	53	1.19
C	130	41	1.28
D	160	23	1.42

^aA 10 wt% polymer suspension was stirred at the temperature indicated for 5 h and then filtered.

and $C_2H_5SO_3H$, but not for H_3PO_4 . They suggested that phosphoric acid interacts with the $-C=N-$ groups through hydrogen bonding rather than salt formation. In any case, the additional phosphoric acid is more weakly tied into the PBI structure, but is still relatively immobile. (In the ^{31}P measurements carried out in the authors' laboratory, magic angle spinning had to be used in order to achieve narrow peak widths.) Still the polymer/acid system is single phase.

2.3 PBI Film-forming methods

Several methods have been reported for forming PBI films doped with phosphoric acid,^[16–20] with polymer modifications to improve physical properties,^[21] and additives to enhance electrode attachment,^[22] and gels^[23] for fuel cell applications. In one method,^[13] the polymer is dissolved in DMAc with 1–2 wt% LiCl added to maintain solution stability. A film is cast on to a glass plate, the solvent is evaporated, and the film is then washed in boiling water to remove the residual LiCl. Doping of the film is accomplished by immersion in phosphoric acid solution. The molarity of the acid determines the final acid loading in the membrane. For example, immersion in 5 M acid solution gives a doping level of about 3 mol of acid per PBI repeat unit (this is termed a 300 mol% doping level). This technique yields a doping level of 520 mol% phosphoric acid by immersion in 11 M acid solution.

In the second method, PBI and acid are directly cast together from a co-solvent, trifluoroacetic acid (TFA).^[19] The solvent is evaporated and the film is ready for use. Even though the compositions are similar, the properties of the film formed by this process are substantially different from those formed by the DMAc method.

2.4 AB-PBI synthesis and membrane formation

AB-PBI is the second basic polymer studied at Case Western Reserve University (CWRU). The polymer is relatively simple to synthesize by a condensation reaction. Figure 2 shows the synthesis route and the chemical structure of the AB-PBI repeat unit. Although the diaminobenzoic acid (DABA) starting material is available commercially, purification is critical for high molecular weight polymer. The highest intrinsic viscosity obtained at CWRU was 7.33 and the preferred reaction conditions were 200 °C for 2 h with a DABA/ P_2O_5 / H_3PO_4 ratio of 1 : 7 : 3.22. Delano *et al.*^[25a] made AB-PBI with a blocking agent, benzoic acid, to limit the molecular weight. Their highest IV, in 0.05% sulfuric acid, was 5.86, with no blocking agent. They calculated that

an IV of 4.1 corresponded to a molecular weight of 71 000, based on the ratio of benzoic acid to monomer used. However, they neglected to consider the impurities originally present. When this was taken into account,^[25b] their highest molecular weight was 39 000. The highest molecular weight polymer made in our laboratory, with $[\eta] = 7.33$, was 53 000. The analysis showed that the molecular weight was proportional to the viscosity to the 0.9 power.^[25b] Reports in the literature^[25c] indicate that much higher molecular weights are achievable (IV up to 15). This would correspond to a molecular weight of about 100 000. Because only a single compound is needed to generate polymer, it is relatively simple to make high viscosity material ($>3 \text{ dl g}^{-1}$) that produces films with good mechanical properties.

AB-PBI is soluble in TFA/ H_3PO_4 under the same conditions as PBI. It was found to be soluble in several alcohols if NaOH or KOH was added. Initial casting was done from an ethanol/NaOH solution in a nitrogen atmosphere. The films were then placed in phosphoric acid solutions in order to dope them. (PBI is also soluble in ethanol/NaOH.) AB-PBI is also soluble in *N*-methylpyrrolidinone/LiCl.

2.5 Mechanical properties of PBI and AB-PBI membranes

The change in mechanical properties with phosphoric acid doping is interesting. Post-doped films increase in modulus and toughness as acid is added up to about one phosphoric acid group per benzimidazole; as more acid is added, the films' moduli decrease. The effect of the doping level on the modulus is shown in Figure 3 for PBI of two different viscosities. X-ray data show that PBI forms a crystalline complex with phosphoric acid, as does AB-PBI.

In the case of TFA films, the toughness (work to break the film, i.e., by integration of the stress–strain curve) of

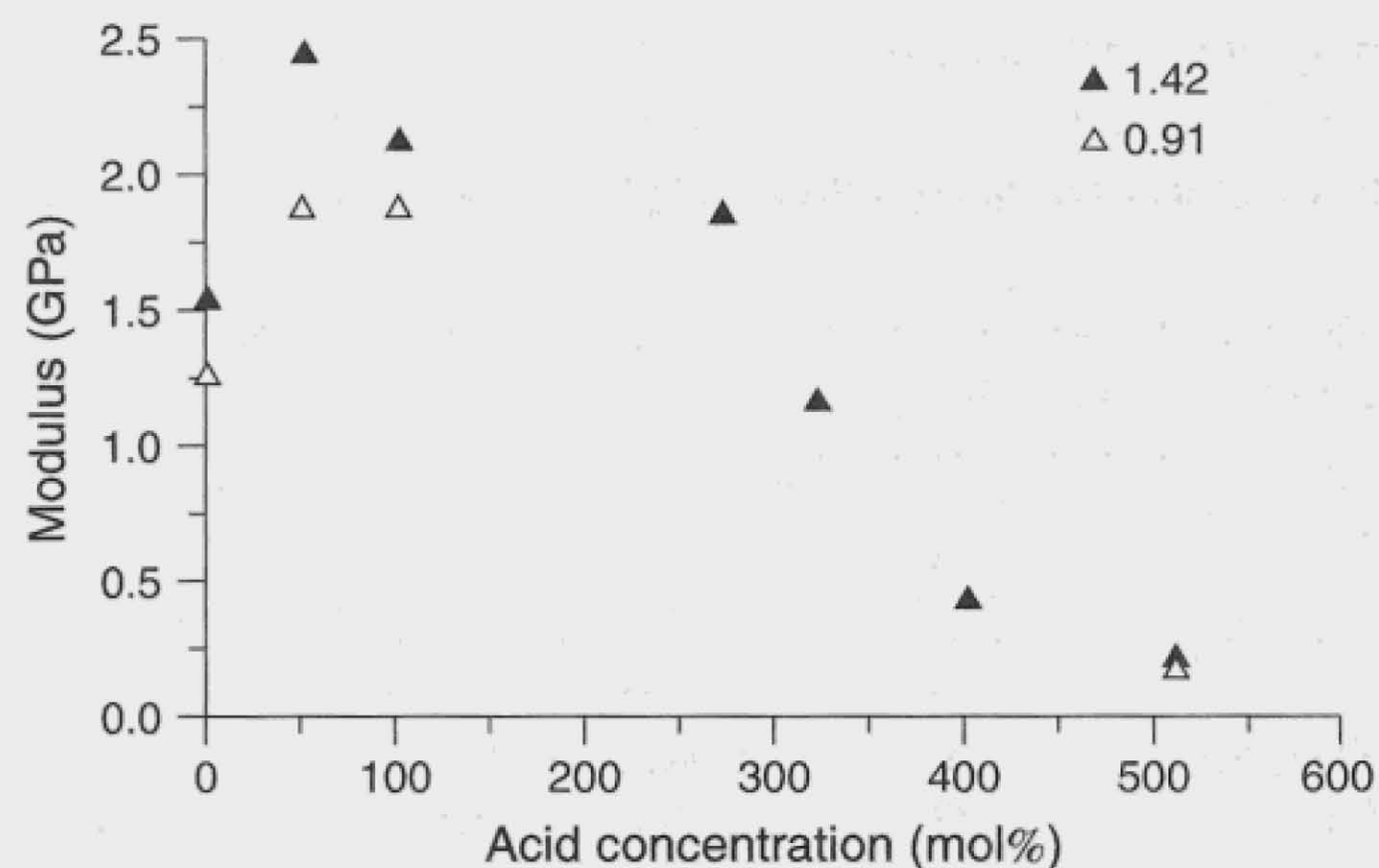


Figure 3. Modulus vs phosphoric acid doping level for PBI films of inherent viscosity 0.91 and 1.42.

the acid-free polymer increases to about 150 MPa for 1.42 IV material compared with 50 for 0.91 IV material. The addition of 50 mol% phosphoric acid drops the toughness to about 100 MPa. As the acid concentration increases, the toughness increases to about 140 MPa since the modulus remains high while ultimate elongation increases. However, once the acid concentration exceeds 200 mol% the excess acid acts as a plasticizer and the toughness decreases (e.g., it drops to about 70 MPa with 500 mol% acid).

Films formed by the DMAc casting method are normally stronger and tougher than those cast from TFA. TFA films require a polymer of higher IV in order to generate films of reasonable strength. TFA films have much more crystallinity than comparably doped DMAc films, and the surface texture is different. TFA films are softer and more rubbery.

The moduli of comparably doped PBI and AB-PBI films are about the same. However, the higher molecular weight attainable with the AB-PBI produces films with greater elongation and toughness than found for PBI. A remarkable property of this material is the amount of strain before break. In a few cases, films have been stretched by a factor of 10 before breaking. The increase in elongation, and therefore toughness, is a direct consequence of the longer chain length.

An issue with post-doped films (i.e., films cast from DMAc) is that they continue to crystallize with further heating. The modulus increases with increasing crystallization, tending to make the films brittle. This was not found when TFA cast films were tested. The modulus remains constant even after heating at 190 °C for a day.

An issue found with the TFA-cast PBI films is their generally low elongation at break. The polymer crystallizes from a relatively dilute solution when it is formed. There is little molecular entanglement at this molecular weight and the film tends to tear easily. Films made using a higher molecular weight polymer should have acceptable properties.

2.6 Chemical stability of PBI and AB-PBI membranes

Samms *et al.*^[26] studied the thermal stability of PBI under simulated fuel cell conditions. Thermogravimetric analysis (TGA) coupled with mass spectrometry (MS) was used with samples of polymer, polymer/acid, and polymer/acid/platinum under environments of air, nitrogen, or 5% hydrogen gas in nitrogen. The gases simulated the fuel cell environment. The high surface area platinum pinned the potential at a strongly oxidizing condition, or a strongly reducing condition. The results indicate that the PBI/phosphoric acid system was stable at temperatures

below 600 °C, with only absorbed water and water from acid dehydration being released. Above 600 °C the decomposition products depended on whether the gas environment was reducing or oxidizing. Although CO₂ emissions were observed at lower temperatures, the amount was small and was attributed to oxidation of impurities and the decomposition of the PBI chain carboxyl end group (450–550 °C).

Kawahar *et al.*^[15] have studied the thermal stability of the PBI and PBI/acid systems using TG/DTA analysis. They found that PBI and PBI/phosphoric acid systems were stable to temperatures in excess of 500 °C. In the case of PBI/sulfuric acid, stability was observed below a temperature of about 300 °C, above which observed decomposition was attributed to elimination of acid molecules. In the authors' laboratory, data shows that at higher acid concentrations, >200 mol%, sulfuric acid catalyzed sulfonation of the benzimidazole ring started at about 200 °C. Below 200 mol%, sulfonation occurred only when the temperature was >300 °C. It is doubtful that acid is lost since it exists as the bisulfate or sulfate ion.

3 IONIC CONDUCTIVITY AND TRANSPORT PROPERTIES OF PBI AND AB-PBI MEMBRANES

3.1 Ionic conductivity

It has been shown that the ionic conductivity of phosphoric acid-doped PBI membranes increases with increasing acid content, RH (at a constant temperature) and temperature (at a constant RH). For a constant water partial pressure, the conductivity is somewhat independent of temperature, as the increase in conductivity due to temperature alone is offset by the decrease in RH. The conductivity of the TFA-cast membranes, which are formed with acid already present in the structure, is significantly greater (2.5–3 times) than that of the DMAc-cast films that were subsequently doped with acid.

Conductivity data under controlled RH are given in Figure 4 for the PBI/phosphoric acid system cast from TFA solutions. At 150 °C and 30% RH or 200 °C and 10% RH, the conductivity of the TFA-cast membranes is similar to that of Nafion[®] at 80 °C and 100% RH. The purpose of controlling the RH is to control the distribution of phosphoric acid species, i.e., H₃PO₄ vs H₄P₂O₇, H₅P₃O₁₀, etc., that occurs with loss of water. Caution must be exercised when examining data in the literature where RH is not controlled since the state of the phosphoric acid may be continually changing and may never reach a true steady state or equilibrium condition. Conductivity measurements reported here were performed using a four-probe apparatus to eliminate

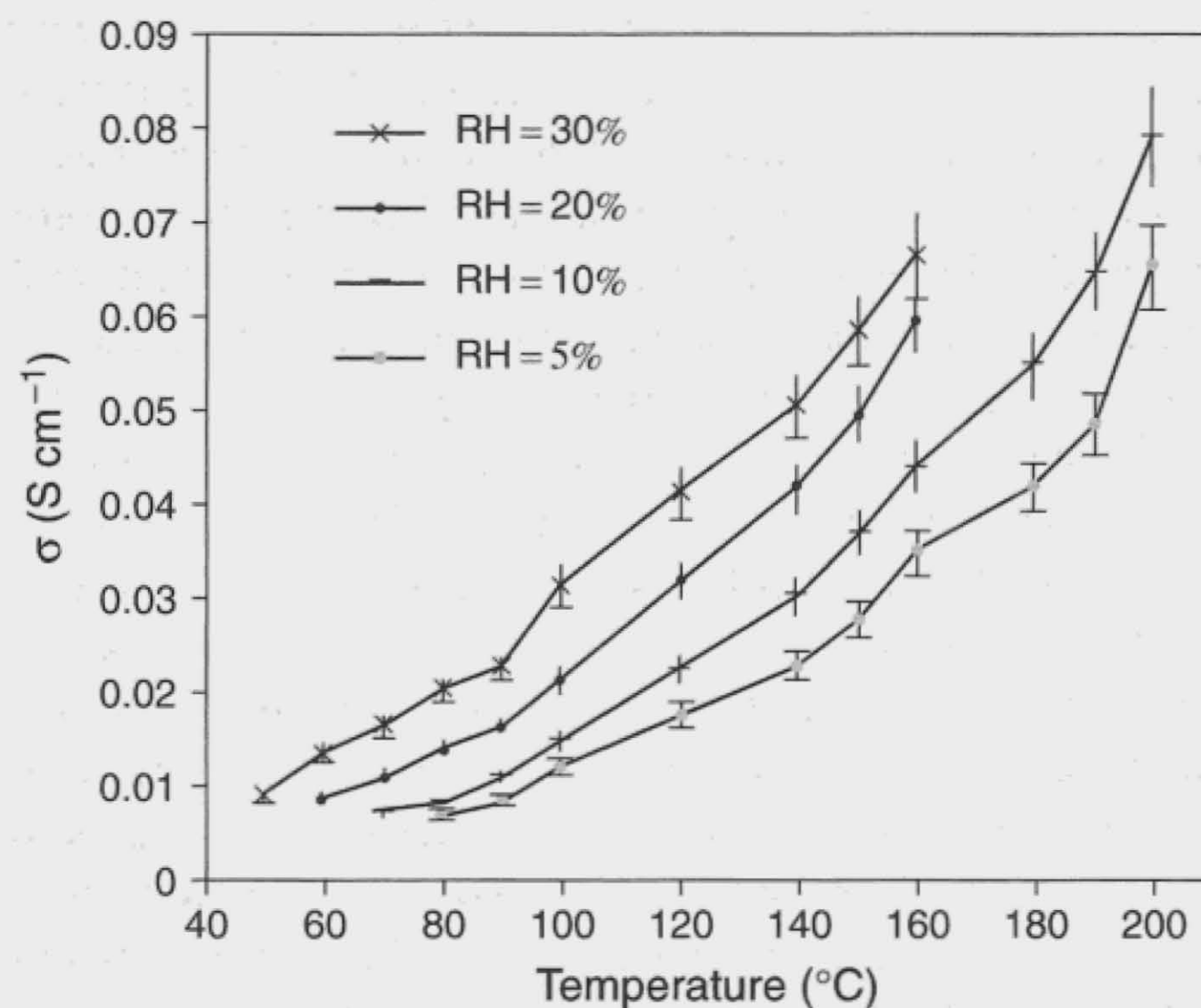


Figure 4. Conductivity of PBI/phosphoric acid cast from TFA, 630 mol% doping level.

interfacial impedances. The apparatus was contained within a sealed stainless-steel vessel, into which water could be injected, and which was placed inside an oven and connected to a gas manifold system. In this manner the temperature, pressure, and humidity could be controlled.

In Figure 5, an Arrhenius plot is given of the data from Figure 4. For each RH, a linear relationship is observed. The activation energies for ionic conduction derived from this data range from 0.5 to 1 eV.

In order to determine the species responsible for the ionic conduction, Hittorf experiments have been performed.^[27] In

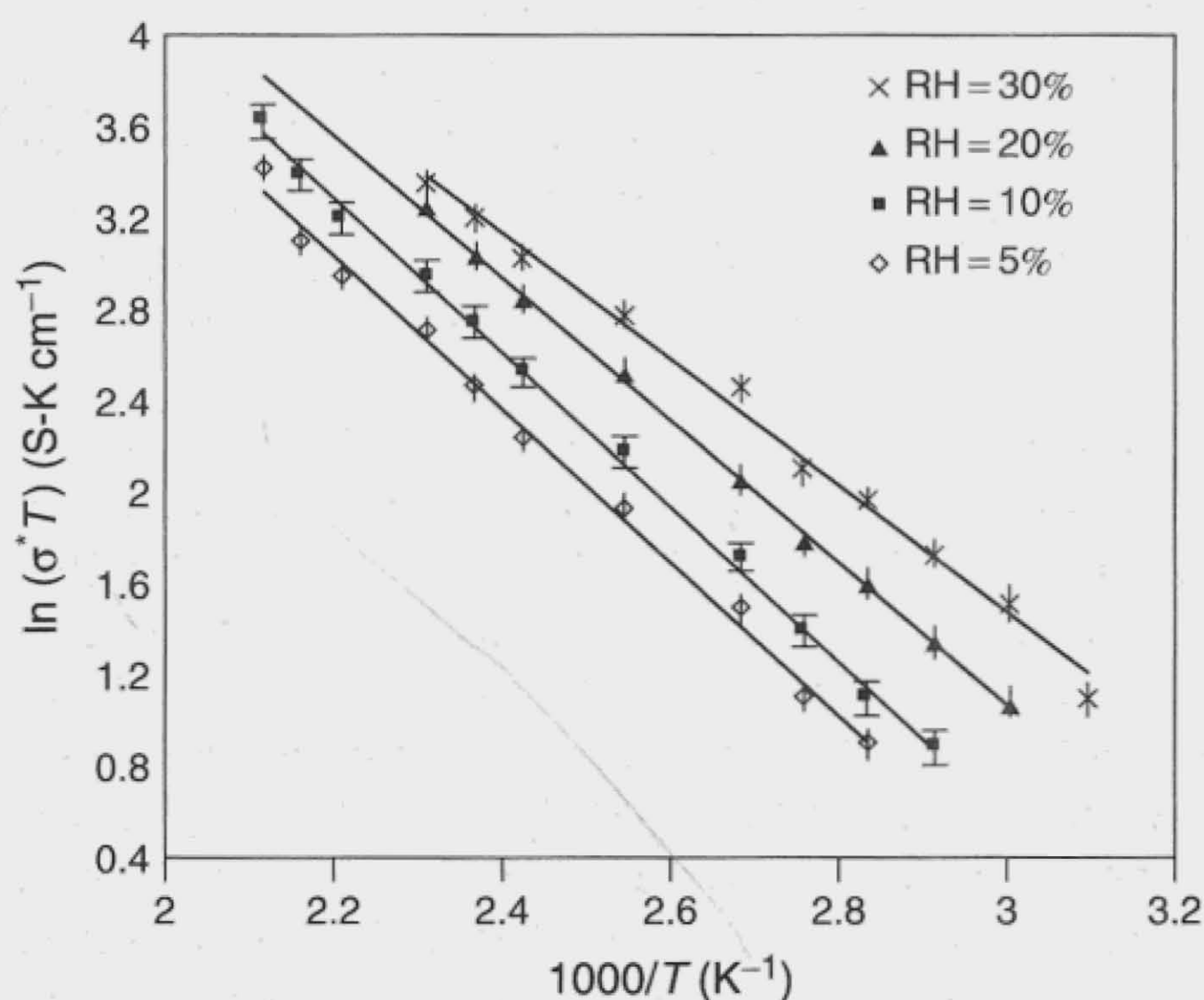


Figure 5. Conductivity data fit with Arrhenius equation, $\sigma T = \sigma_0 \exp(-E_A/kT)$, for the data given in Figure 4 for a 630 mol% phosphoric acid doping level.

these experiments, a quantity of charge is passed through a strip of sample, which is then sectioned, and the composition of each section is determined. Based on the measured phosphorus/carbon and phosphorus/nitrogen ratios, the results of these experiments show that the transference number for a dihydrogenphosphate anion in the PBI/H₃PO₄ electrolyte (DMAc cast) is ca. 0.02. The proton transference number was found to be ca. 0.98 (because of experimental error, it may be higher). Dippel *et al.*^[28] have reported that orthophosphoric acid dissociation in concentrated phosphoric acid accounts for 2.6% of the conduction, and Grotthus conduction accounts for 97.4% of the current. Chung *et al.*^[29] came to a similar conclusion, but with an even higher proton transfer number of 0.99. Since most of the current is carried by the protons in the PBI/phosphoric acid system, it is unlikely that redistribution of H₃PO₄ will adversely affect fuel cell operation.

Fontenella *et al.*^[30] and Bouchet *et al.*^[31] have estimated activation volumes in the PBI/acid system by measuring the conductivity as a function of pressure. Values on the order of 4–10 cm³ mol⁻¹ indicate that conductivity involves small species such as protons. Bouchet *et al.*^[31] have suggested that the high value of the activation entropy is consistent with a Grotthus mechanism involving a protonated imide site and a counterion such as H₂PO₄⁻ or HSO₄⁻. The activation energy range (0.5–1 eV) for the data shown in Figure 5 is consistent with the range of activation energies of 0.68 eV for phosphoric acid-doped PBI and 1.08 eV for sulfuric acid-doped PBI estimated by Bouchet *et al.*^[31] Bouchet and Siebert^[14] found the activation energy to be 0.8–0.9 eV for PBI/phosphoric acid independent of acid concentration. However, for PBI/sulfuric acid the activation energy was found to be ca. 0.5 eV for 3.2 acids per repeat unit, but 1 eV when there was less than one acid per repeat unit. These differences in the concentration dependency of activation energy suggest that PBI/phosphoric acid is an ideal solution, whereas PBI/sulfuric acid is not. No explanation for this difference was given. However, there is no reason for the activation energy for conduction to be the same for a bisulfate/sulfuric acid system versus a sulfate/bisulfate system. The increase in activation energy with lower acidity is expected. Using NMR pulse gradient spin-echo measurements, Chung *et al.*^[29] reported higher activation energies (0.38 eV) for the slower phosphorus diffusion as opposed to lower activation energy (0.26 eV) for proton hopping.

Conductivity of the AB-PBI system has also been measured for conditions similar to those in Figure 4. Note that the 300% phosphoric acid level in AB-PBI is equivalent (in terms of acid molecules per benzimidazole) to a 600% acid level in PBI, which has two benzimidazole groups per

polymer repeat unit. For an equivalent doping level the conductivity of the AB-PBI films is roughly 20% greater than that of the PBI films across the range of conditions shown in Figure 4. There are two possible explanations for the higher conductivity of doped AB-PBI films compared with the doped PBI films. They may be acting together. First, the simpler structure may allow the AB-PBI/phosphoric acid complex to reach higher crystallinity compared with the PBI complex. The crystalline phase rejects excess phosphoric acid, generating an acid-rich amorphous phase. This explanation is certainly true when comparing the post-doped PBI films versus the TFA-cast films. Second, AB-PBI has a lower molecular weight per benzimidazole group than PBI. This means that the same doping ratio, AB-PBI has a greater weight fraction of acid than does PBI. At 3.0 acid molecules per benzimidazole, the acid weight fraction is 71% for AB-PBI vs 66% for PBI. This should lead to higher conductivity for AB-PBI films.

3.2 Electroosmotic water drag

The electroosmotic drag of water that accompanies proton transport from anode to cathode is an important parameter when evaluating polymer electrolytes. Excessive water drag can lead to an imbalance of water within the cell, resulting in dehydration of the anode and loss of conductivity and/or flooding of the cathode. The electroosmotic drag coefficient has been determined for the PBI/H₃PO₄ electrolyte, using a hydrogen pump cell in which the total flux of hydrogen and osmotically dragged water is directly measured.^[32] These measurements were performed with DMAc-cast membranes as a function of temperature, humidity, and current density. The combined drag fluxes of water and methanol have also been investigated.

Weng *et al.* have reported^[32] that the electroosmotic drag coefficient for water and methanol was essentially zero under all conditions. (Although the values may not be

actually zero, the experimental method could not reliably distinguish drag coefficients smaller than 0.1, and most experiments indicated less than 0.01.) In other words, the water balance problems (dehydration near the anode and/or cathode flooding) typically associated with PEM fuel cells using perfluorosulfonic acid membranes will not occur in fuel cells utilizing doped PBI membranes.

3.3 Methanol permeation

Methanol crossover rates through doped PBI membranes (DMAc cast) have been determined by direct measurement of the methanol permeability, by a methanol sorption technique, and by real-time analysis of the cathode exhaust stream of an operating fuel cell using mass spectrometry.^[33] Each of these measurements yielded crossover rates of the order of 10 mA cm⁻² for 3 mil (0.0075 cm) thick films. The MS results are summarized in Table 3. These experiments were performed at 180 °C using operating fuel cells. For these studies the mass spectrometer was used to determine the CO₂ partial pressure in the cathode exhaust, using the mass signal for *m/z* 44. Assuming 100% oxidation of methanol to CO₂ in the cathode, the CO₂ signal is then proportional to the methanol flux. The CO₂ partial pressure was inversely proportional to the air flow rate into the cathode, indicating a constant methanol flux. With the cell at open circuit, the methanol crossover rate increased with a decrease in the water/methanol ratio in the anode feed stream, as expected.

Similar measurements were made with the cell on load. These results are shown in Table 3 and indicate a slight increase in CO₂ in the cathode exhaust as the current is increased. For these measurements, the anode was fed an H₂/H₂O/CH₃OH mixture. Sufficient hydrogen was fed to the cell to support the current passed, so it can be safely assumed that no CO₂ was generated at the anode; the CO₂ collected at the cathode is purely

Table 3. Estimate of methanol drag coefficient from mass spectrometric data under load.^a

Current density (mA cm ⁻²)	Methanol flux detected as CO ₂ (M s ⁻¹ cm ⁻²)	Drag coefficient: CH ₃ OH/H ⁺	Crossover rate due to drag (mA cm ⁻²)
100	4.3 × 10 ⁻⁹	0.0042	2.5
150	5.5 × 10 ⁻⁹	0.0035	3.2
200	7.0 × 10 ⁻⁹	0.0034	4.1
250	7.4 × 10 ⁻⁹	0.0029	4.4
300	9.3 × 10 ⁻⁹	0.0030	5.4

^aDMAc-cast PBI membranes (500 mol% H₃PO₄), 0.011 cm thick. Temperature, 180 °C. All measurements at atmospheric pressure. Anode gas composition: 50 mol% H₂, 35 mol% CH₃OH, 15 mol% H₂O.

from methanol crossover. The crossover rate increased with increasing current, indicating a small electroosmotic drag of methanol associated with proton transfer. The total methanol crossover due to drag and concentration driven permeation is ca. 15 mA cm^{-2} .

4 ELECTROCHEMICAL BEHAVIOR

4.1 Hydrogen fuel cells

Some early work demonstrating an H_2/O_2 PBI fuel cell was reported by Wang *et al.*^[34] The results showed no membrane deterioration after a 200 h test at 150°C . The maximum power was 0.25 W cm^{-2} at 700 mA cm^{-2} with atmospheric pressure hydrogen and oxygen without humidification. These results were obtained with 4 mil (0.01 cm) thick DMAc-cast membranes. Although not impressive, it needs to be noted that the electrode development has just started.

More recent H_2/O_2 fuel cell results presented by Samms^[5] using lower Pt loadings ($0.35 \text{ mg Pt cm}^{-2}$ on each electrode) and TFA-cast membranes (3 mil, 0.0075 cm thick) evaluated the effects of temperature and anode feed gas composition (H_2 , $\text{H}_2/25\% \text{ CO}_2$, $\text{H}_2/25\% \text{ CO}_2/1\% \text{ CO}$) at atmospheric pressure and without humidification. The maximum power density reported was ca. 0.4 W cm^{-2} at 0.5 V. The power output rose with temperature, reaching a broad plateau between 175 and 225°C . The addition of 1% CO to the hydrogen stream was observed to decrease the cell potential by 17 mV at 600 mA cm^{-2} at 200°C .

Hydrogen/oxygen fuel cell results obtained with phosphoric acid-doped PBI membranes have been reported by Qingfeng *et al.*^[35] A power density of nearly 0.5 W cm^{-2} (at ca. 0.5 V) was reported for a membrane doped to 650 mol%, operating at 190°C on atmospheric pressure H_2 and O_2 . The power output increased substantially as the temperature was increased from 55 to 190°C .

Savadozo and Xing^[36] have also reported H_2/O_2 fuel cell results between 50 and 185°C at atmospheric pressure using sulfuric and phosphoric acid-doped PBI. A maximum power output of 0.65 W cm^{-2} was reported. They found that the addition of 3% CO to the hydrogen feed had no effect on the polarization curves at 185°C .

Various industrial groups have informally reported H_2/air fuel cell performance of the order of $0.25\text{--}0.4 \text{ W cm}^{-2}$. Unfortunately, the details of these experiments are kept confidential.

4.2 Direct methanol fuel cells

A DMFC using a DMAc-cast membrane has been reported by Wang *et al.*^[37] In that work, the anode was a 4 mg cm^{-2}

Pt/Ru alloy catalyst, and the cathode was Pt black with the same loading. Using first-generation electrodes, the authors demonstrated a 0.1 W cm^{-2} power level at 200°C at 0.4 V operating on air and a 1:1 mixture of methanol and water at atmospheric pressure. Previously unreported DMFC data obtained with TFA-cast membranes are reported here. Platinum black (Johnson-Matthey) and platinum/ruthenium alloy (Giner) were used as catalysts for oxygen reduction and methanol oxidation, respectively. The measurements were performed at 200°C and atmospheric pressure and a water to methanol mole ratio of 2:1 was used as the anode feed. The maximum power density obtained with the TFA cast membrane was ca. 0.2 W cm^{-2} at 0.4 V. The increased power output was primarily due to lower iR losses. The open-circuit potentials of the DMAc- and TFA-cast cells were essentially the same (0.75–0.78 V). This indicates that the methanol crossover effect on the cathode is the same for both membranes, and that the enhanced conductivity of the TFA-cast membranes did not promote higher methanol permeability.

The effect of temperature ($150\text{--}200^\circ\text{C}$) on DMFC performance has been evaluated using DMAc-cast membranes and an anode feed (water/methanol mole ratio) of 2:1. As the temperature was increased, the open-circuit voltage of the cells increased from 0.63 to 0.75 V. The increase observed is due primarily to a lower crossover rate; methanol is less soluble in the electrolyte at higher temperatures. The voltage under load also increased over a broad range of current density as the cell temperature increased. At 250 mA cm^{-2} , the voltage gain was approximately 75 mV over the range of temperature considered. The increased performance with increasing temperature can be attributed to lower methanol crossover and higher electrolyte conductivity. Surprisingly, the performance of the methanol anode did not significantly improve with increasing temperature. This may be due to the lower methanol solubility in the electrolyte at higher temperatures offsetting the expected kinetic improvement. The effect of varying water to methanol ratios in the anode feed has also been determined for the mole ratio range of 1:1 to 4:1. It was found that increasing the water content significantly improves the overall performance of the fuel cell. For water to methanol ratios of up to at least 4:1, the gains in the cathode performance (as a result of lower methanol crossover) and in conductivity (due to higher humidity) are greater than the loss in anode performance (as a result of lower methanol concentration). For water to methanol ratios of 2:1 or higher, CO_2 is the predominant product (>97%). At a stoichiometric water:methanol ratio of 1:1, the product distribution was CO_2 (80–90%) and roughly equal parts of methyl formate and methanaldimethylacetal [$\text{H}_2\text{C}(\text{OCH}_3)_2$]. Both of the minor products are likely

the result of electrochemical/chemical mechanisms, e.g., oxidation of methanol to formic acid, followed by acid-catalyzed reaction of formic acid with methanol to form methyl formate.

4.3 Other direct oxidation fuel cells

Wang *et al.*^[38] have reported the electrooxidation of ethanol, 1-propanol and 2-propanol in a phosphoric acid-doped PBI fuel cell at 170 °C with Pt/Ru alloy as the anode catalyst. MS was used to determine the anode reaction product distribution. The polarization behavior of ethanol was similar to that of methanol (ca. 0.1 W cm⁻²); however, ethanal (acetaldehyde) was the main reaction product. Higher CO₂ yields were obtained with higher water/ethanol ratios in the feed. 1-Propanol and 2-propanol oxidation yielded mainly propanal and acetone, respectively; the electrochemical activity of these fuels was low. Wang *et al.*^[39] also examined trimethoxymethane as an alternative fuel in a PBI fuel cell.

Savadogo and Rodriguez Varela^[40] have reported the direct oxidation of propane in a sulfuric acid-doped PBI fuel cell. They claimed complete oxidation of propane to CO₂ at 95 °C using a Pt/CrO₃ catalyst. The maximum power density was reported to be 0.046 W cm⁻² using oxygen as the oxidant.

5 ISSUES

The PBI/dihydrogenphosphate acid electrolyte is less than ideal for electrochemical fuel cell reactions. The phosphoric anion is known to adsorb strongly on platinum surfaces, thus slowing the kinetics of surface reactions, especially the reduction of oxygen. Oxygen reduction on a PBI-coated platinum disk electrode in dilute acid solution has been studied by Zecevic *et al.*^[41] They found that, as expected, the rate of oxygen reduction was significantly lowered in phosphoric acid compared with a non-adsorbing anion such as that of perchloric acid. However, the Tafel slope was the same for the two electrolytes, indicating no change in the mechanism of the reaction. There was little, if any, effect on the rate of reaction due the presence of the PBI film on the platinum surface in phosphoric acid electrolyte. Qingfeng *et al.*^[35] have also studied the oxygen reduction reaction, but at high temperatures using gas diffusion electrodes. The results indicated that PBI actually enhanced the oxygen reduction reaction. Although the reason for this is not clear, it is thought that the enhanced rate is at least partially due to increased oxygen solubility in PBI.

Another issue with PBI/phosphoric acid electrolyte for fuel cell applications is the fact that liquid water can leach the acid from the membrane, leaving only about two acid molecules per repeat unit. The conductivity of the membrane will decrease as acid is extracted. Even if a fuel cell is operated at temperatures above water condensation, this could lead to serious problems during fuel cell start-up, as well as for long-term stability. Akita *et al.*^[42] have examined organic phosphoric acid analogs to address this problem. The notion was to increase the acid hydrophobicity and thus lessen the leachability of the acid by aqueous solutions. They showed that 60% of diphenylphosphoric acid remained in a membrane initially doped with five acid molecules per repeat unit after attempting to extract with 1 M methanol solution at 85–90 °C. This compares with only 32% remaining for an equivalent system, PBI doped with phosphoric acid. Of course, further improvements in stability are desirable.

6 OTHER BASIC POLYMERS

Several other acid-doped basic polymers have been investigated as potential electrolytes for fuel cell applications. In studies reported by Hasiotis *et al.*^[43–45], blends of PBI and sulfonated polysulfones were doped with phosphoric acid. The conductivities for the blends were reported to exceed those of the PBI/phosphoric acid system. In addition, the blend offers potentially better mechanical properties for films.^[45] The desired composition will depend on the trade-off between conductivity and mechanical properties. Bozkurt *et al.*^[46] examined the phosphoric acid-doped PAMA⁺ H₂PO₄⁻·xH₂O system when *x* varied from 0.5 to 2.0. Tsuruhara *et al.*^[47] have studied phosphoric acid poly(silamine) (PSA). Both of these systems have proton conductivities at practical levels under certain conditions.

7 SUMMARY

The results shown here indicate that the expected benefits of elevated-temperature fuel cells (enhanced tolerance to carbon monoxide, greatly reduced humidification issues) can be realized in a polymer electrolyte system. However, it is clear that other significant issues remain, including electrode structure optimization and membrane optimization for optimal conductivity, mechanical properties, and stability against acid leaching. It is also apparent that fundamental questions relating to the mechanisms for conduction and for oxygen reduction in these electrolytes remain open. These areas will need to be addressed in order to realize the potential benefits in a commercially viable system.

ACKNOWLEDGEMENTS

The authors are grateful to the numerous students, research associates, and visiting scholars whose work is summarized in this chapter and much of which, but not all, appear in the publications referenced. They especially acknowledge the unpublished recent measurements of Mr Yulin Ma reported here on the conductivity of the PBI/phosphoric acid system, which is the subject of his PhD dissertation research. Portions of this work were supported by the US Defense Advanced Research Projects Agency (DARPA) and the US Department of Energy (DOE).

REFERENCES

- (a) Y. Sone, P. Ekdunge and D. Simonsson, *J. Electrochem. Soc.*, **143**, 1254 (1996); (b) G. Alberti, M. Casciola, L. Massinelli and B. Bauer, *J. Membr. Sci.*, **185**, 73 (2001).
- T. E. Springer, T. A. Zawodzinski and S. Gottesfeld, *J. Electrochem. Soc.*, **138**, 2363 (1991).
- R. Lemons, *J. Power Sources*, **29**, 251 (1990).
- C. Yang, P. Costamagna, S. Srinivasan, J. Benziger and A. B. Bocarsly, *J. Power Sources*, **103**, 1 (2001).
- S. Samms, 'Kinetics in an Internal Reforming Fuel Cell, High Temperature PEM Fuel Cell Performance, and a Fundamentals Based Impedance Model', PhD Dissertation, Case Western Reserve University, Cleveland, OH (2001).
- N. Miyaki, J. S. Wainright and R. F. Savinell, *J. Electrochem. Soc.*, **148**, A898 (2001).
- N. Miyaki, J. S. Wainright and R. F. Savinell, *J. Electrochem. Soc.*, **148**, A905 (2001).
- S. J. Lee, K. T. Adjemian, A. B. Bocarsly and S. Srinivasan, in 'Extended Abstracts of the Electrochemical Society', Vol. 2000-1, Toronto Meeting, May 14-18, 2000, Abstract 85 (2000).
- C. Yang, S. Srinivasan, A. S. Arico, P. Creti, V. Baglio and V. Antonucci, *Electrochem. Solid-State Lett.*, **4**, A31 (2001).
- R. F. Savinell, E. Yeager, D. Tryk, U. Landau, J. Wainright, D. Weng, M. Litt and C. Rogers, *J. Electrochem. Soc.*, **141**, L46 (1994).
- S. Wasmus, A. Valeriu, G. D. Mateescu, D. A. Tryk and R. F. Savinell, *Solid State Ionics*, **80**, 87 (1995).
- R. F. Savinell and M. H. Litt, US Patent 5,525,436 (1996).
- J. S. Wainright, J.-T. Wang, D. Weng, R. F. Savinell and M. Litt, *J. Electrochem. Soc.*, **142**, L121 (1995).
- R. Bouchet and E. Siebert, *Solid State Ionics*, **118**, 287 (1999).
- M. Kawahara, J. Morita, M. Rikukawa, K. Sanui and N. Ogata, *Electrochim. Acta*, **45**, 1395 (2000).
- G. Calundann and T. S. Chung, US Patent 5,091,087 (1992).
- F. J. Onorato, M. J. Sansone, D. W. Kim, S. M. French and F. Marikar, US Patent 6,042,968 (2000).
- M. J. Sansone, F. J. Onorato, S. M. French and F. Marikar, US Patent 6,187,231 (2001).
- (a) M. H. Litt and R. F. Savinell, US Patent 5,716,727 (1998); (b) R. F. Savinell and M. H. Litt, US Patent 6,025,085, (2000); (c) R. F. Savinell and M. H. Litt, US Patent 6,099,988 (2000).
- F. J. Onorato, M. J. Sansone, D. W. Kim, S. M. French and F. Marikar, US Patent 6,042,968 (2000).
- M. J. Sansone, F. J. Onorato and N. Ogata, US Patent 5,599,639 (1997).
- W. Han, C. Li and K. K. Lian, US Patent 5,723,231 (1998).
- F. J. Onorato, M. J. Sansone, S. M. French and F. Marikar, US Patent 5,945,233 (1999).
- (a) R. Ameri, 'Polybenzimidazole film containing phosphoric acid as a proton exchange membrane (PEM)', PhD Dissertation, Case Western Reserve University, Cleveland, OH (1997); (b) M. Litt, R. Ameri, Y. Wang, R. Savinell and J. Wainright, *Mater. Res. Soc. Symp. Proc.*, **548**, 313 (1999).
- (a) C. B. Delano, R. R. Doyle and R. J. Milligan; *Technical Report AFML-TR-74-22* (1974); (b) Y. Wang, 'The Synthesis and Properties of Poly(2,5-benzimidazole)', MS Thesis, Case Western Reserve University, Cleveland, OH (1998); (c) A. Wereta Jr and M. T. Gehetia, *Polym. Eng. Sci.*, **18**, 204 (1978).
- S. R. Samms, S. Wasmus and R. F. Savinell, *J. Electrochem. Soc.*, **143**, 1225 (1996).
- D. Weng, 'Water and Methanol Transport in Polymer Electrolytes for Elevated Temperature Fuel Cells', PhD Dissertation, Case Western Reserve University, Cleveland, OH (1996).
- Th. Dippel, K. D. Kreuer, J. C. Lassegues and D. Rodriguez, *Solid State Ionics*, **61**, 41 (1993).
- S. H. Chung, S. Bajue and S. G. Greenbaum, *J. Chem. Phys.*, **112**, 8515 (2000).
- J. J. Fontanella, M. C. Wintersgill, J. S. Wainright and R. F. Savinell, *Electrochim. Acta*, **43**, 1289 (1998).
- P. Bouchet, S. Miller, M. Duclot and J. L. Souquet, *Solid State Ionics*, **145**, 69 (2001).
- D. Weng, J. S. Wainright, U. Landau and R. F. Savinell, *J. Electrochem. Soc.*, **143**, 1260 (1996).
- S. Wasmus, J.-T. Wang and R. F. Savinell, *J. Electrochem. Soc.*, **143**, 1233 (1996).
- J.-T. Wang, R. F. Savinell, M. H. Litt and H. Yu, *Electrochim. Acta*, **41**, 193 (1996).
- L. Qingfeng, H. A. Hjuler and N. J. Bjerrum, *Electrochim. Acta*, **45**, 4219 (2000).
- O. Savadogo and B. Xing, *J. New Mater. Electrochem. Syst.*, **3**, 345 (2000).
- J.-T. Wang, J. S. Wainright, R. F. Savinell and M. H. Litt, *J. Appl. Electrochem.*, **26**, 751 (1996).
- J.-T. Wang, S. Wasmus and R. F. Savinell, *J. Electrochem. Soc.*, **142**, 4218 (1995).
- J.-T. Wang, W. F. Lin, M. Weber, S. Wasmus and R. F. Savinell, *Electrochim. Acta*, **43**, 3821 (1998).

40. O. Savadogo and F. J. Rodriguez Varela, *J. New Mater. Electrochem. Syst.*, **4**, 93 (2001).
41. (a) S. K. Zecevic, S. Gojkovic, J. S. Wainright and R. F. Savinell, *J. Electrochem. Soc.*, **144**, 2973 (1997); (b) S. K. Zecevic, J. S. Wainright, M. H. Litt and R. F. Savinell, *J. Electrochem. Soc.*, **145**, 3308 (1998).
42. H. Akita, M. Ichikawa, K. Nosaki, H. Oyanagi and M. Iguchi, US Patent 6,124,060 (2000).
43. C. Hasiotis, L. Qingfeng, V. Deimede, J. K. Kallitsis, C. G. Kontoyannis and J. J. Bjerrum, *J. Electrochem. Soc.*, **148**, A513 (2001).
44. C. Hasiotis, V. Deimede and C. Kontoyannis, *Electrochim. Acta*, **46**, 2401 (2001).
45. V. Deimede, G. A. Voyiotzis, J. K. Kallitsis, L. Qingfeng and J. J. Bjerrum, *Macromolecules*, **33**, 7609 (2000).
46. A. Bozkurt, M. Ise, K. D. Kreuer, W. H. Meyer and G. Wegner, *Solid State Ionics*, **125**, 225 (1999).
47. K. Tsuruhara, M. Rikukawa, K. Sanui, N. Ogata, Y. Nagasaki and M. Kata, *Electrochim. Acta*, **45**, 1391 (2000).